Electronic Supplementary Material (ESI) for Physical Chemistry Chemical Physics.

Supporting Information:

Accurate Reproducing Kernel-Based Potential Energy Surfaces for the Triplet Ground States of N_2O and Dynamics for the N+NO$\leftrightarrow$O+N_2 and N_2+O$\rightarrow$2N+O Reactions

Debasish Koner,[1] Juan Carlos San Vicente Veliz,[1] Raymond J. Bemish,[2] and Markus Meuwly[1]

[1)] *Department of Chemistry, University of Basel, Klingelbergstrasse 80, CH-4056 Basel, Switzerland*

[2)] *Air Force Research Laboratory, Space Vehicles Directorate, Kirtland AFB, New Mexico 87117, USA*

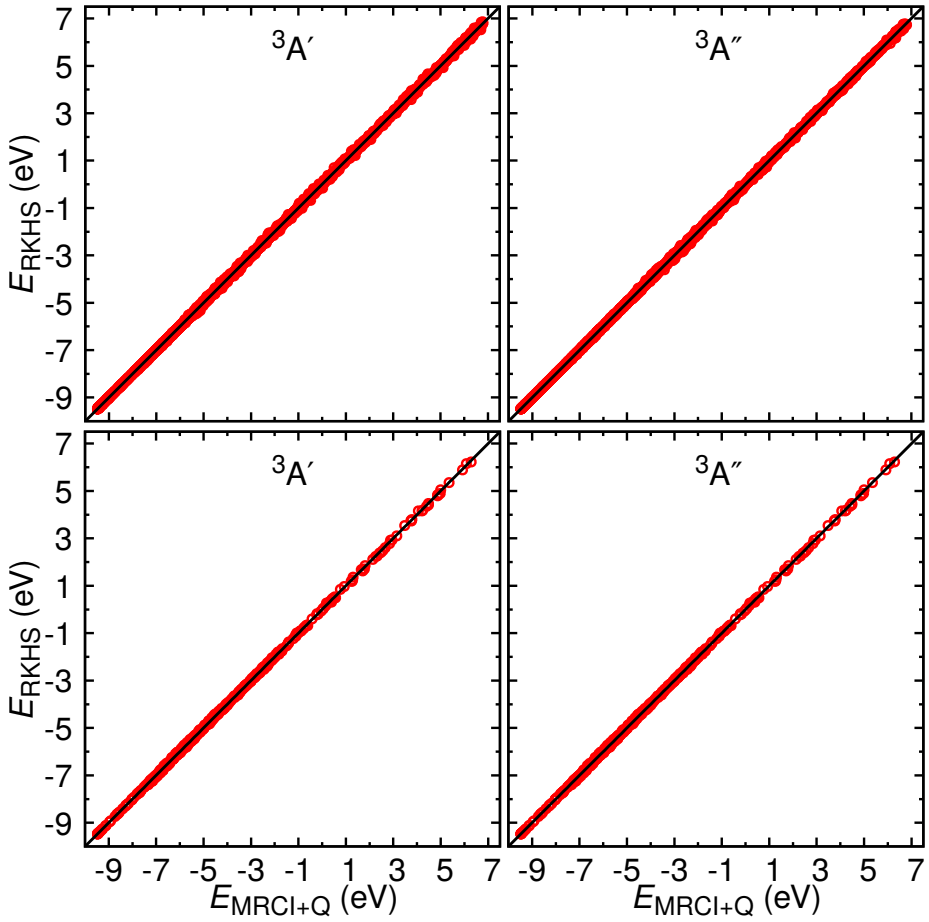

FIG. S1. Correlation between the *ab initio* and RKHS interpolated energies for the training grid (upper panel) and for the test grid (which are not part of the training grid) (lower panel) for ^{3}A′ and ^{3}A″ different electronic states of N_2O. Zero of energy is set to the atomization energy of N_2O i.e., energy of N(^{4}S)+N(^{4}S)+O(^{3}P). The values of R^2 in upper panels for the grid energies up to 6.80 eV are 0.99995 and 0.99996 for ^{3}A′ and ^{3}A″, respectively where as in lower panel for the test grid values of R^2 are 0.99985 and 0.99988 for ^{3}A′ and ^{3}A″, respectively. The correlation for the "on grid points" is not 1 because a) a finite regularization parameter was used (see main text) and b) the global PES is generated by accumulating the weighted contributions from the three channels.

TABLE S1. Rate coefficients for the $N(^4S)$ + $NO(X^2\Pi) \rightarrow O(^3P)$ + $N_2(X^1\Sigma)$ from 100 to 20000 K calculated using QCT on the $^3A'$ and $^3A''$ PESs. Units are in $cm^3s^{-1}molecule^{-1}$

T (K)	$k_1^f(^3A')$	$k_1^f(^3A'')$	$k_1^f(^3A') + k_1^f(^3A'')$
100	0.000	4.879×10^{-11}	4.879×10^{-11}
200	0.000	3.928×10^{-11}	3.928×10^{-11}
300	0.000	3.333×10^{-11}	3.333×10^{-11}
500	9.743×10^{-16}	2.837×10^{-11}	2.837×10^{-11}
800	2.424×10^{-14}	2.592×10^{-11}	2.595×10^{-11}
1000	7.984×10^{-14}	2.590×10^{-11}	2.598×10^{-11}
2000	1.257×10^{-12}	2.871×10^{-11}	3.000×10^{-11}
3000	3.759×10^{-12}	3.234×10^{-11}	3.610×10^{-11}
3500	5.268×10^{-12}	3.458×10^{-11}	3.985×10^{-11}
4000	7.117×10^{-12}	3.609×10^{-11}	4.321×10^{-11}
4500	8.495×10^{-12}	3.816×10^{-11}	4.666×10^{-11}
5000	1.077×10^{-11}	4.018×10^{-11}	5.095×10^{-11}
5500	1.273×10^{-11}	4.100×10^{-11}	5.373×10^{-11}
6000	1.465×10^{-11}	4.290×10^{-11}	5.755×10^{-11}
7500	2.121×10^{-11}	4.776×10^{-11}	6.897×10^{-11}
10000	3.157×10^{-11}	5.516×10^{-11}	8.674×10^{-11}
12500	4.014×10^{-11}	6.095×10^{-11}	1.011×10^{-10}
15000	4.884×10^{-11}	6.793×10^{-11}	1.168×10^{-10}
17500	5.508×10^{-11}	7.087×10^{-11}	1.259×10^{-10}
20000	6.025×10^{-11}	7.524×10^{-11}	1.355×10^{-10}

TABLE S2. Rate coefficients for the $N_A(^4S) + N_BO(X^2\Pi) \rightarrow N_B(^4S) + N_AO(X^2\Pi)$ from 100 to 20000 K calculated using QCT on the $^3A'$ and $^3A''$ PESs. Units are in $cm^3s^{-1}molecule^{-1}$

T (K)	$k_2^f(^3A')$	$k_2^f(^3A'')$	$k_2^f(^3A') + k_2^f(^3A'')$
100	0.000	0.000	0.000
200	0.000	0.000	0.000
300	0.000	0.000	0.000
500	0.000	0.000	0.000
800	0.000	0.000	0.000
1000	0.000	0.000	0.000
2000	1.881×10^{-16}	0.000	1.8812×10^{-16}
3000	2.591×10^{-14}	3.029×10^{-14}	5.6202×10^{-14}
3500	6.513×10^{-14}	9.275×10^{-14}	1.5792×10^{-13}
4000	1.469×10^{-13}	1.718×10^{-13}	3.1872×10^{-13}
4500	2.848×10^{-13}	3.062×10^{-13}	5.9102×10^{-13}
5000	4.408×10^{-13}	4.768×10^{-13}	9.1752×10^{-13}
5500	7.233×10^{-13}	7.878×10^{-13}	1.5112×10^{-12}
6000	1.051×10^{-12}	1.086×10^{-12}	2.1372×10^{-12}
7500	2.626×10^{-12}	2.512×10^{-12}	5.1392×10^{-12}
10000	6.338×10^{-12}	6.481×10^{-12}	1.2822×10^{-11}
12500	1.187×10^{-11}	1.117×10^{-11}	2.3042×10^{-11}
15000	1.696×10^{-11}	1.650×10^{-11}	3.3452×10^{-11}
17500	2.176×10^{-11}	2.106×10^{-11}	4.2812×10^{-11}
20000	2.618×10^{-11}	2.532×10^{-11}	5.1502×10^{-11}

TABLE S3. Rate coefficients for the $O(^3P) + N_2(X^1\Sigma) \rightarrow N(^4S) + NO(X^2\Pi)$ from 2800 to 20000 K calculated using QCT on the $^3A'$ and $^3A''$ PESs. Units are in $cm^3s^{-1}molecule^{-1}$

T (K)	$k^b(^3A')$	$k^b(^3A'')$	$k^b(^3A') + k^b(^3A'')$
2800	0.000	0.000	0.000
3000	0.000	7.605×10^{-16}	7.605×10^{-16}
3500	2.357×10^{-16}	3.824×10^{-15}	4.059×10^{-15}
4000	3.782×10^{-15}	1.764×10^{-14}	2.142×10^{-14}
4500	1.026×10^{-14}	5.161×10^{-14}	6.187×10^{-14}
5000	3.082×10^{-14}	1.191×10^{-13}	1.499×10^{-13}
5500	8.772×10^{-14}	2.555×10^{-13}	3.433×10^{-13}
6000	1.575×10^{-13}	4.374×10^{-13}	5.950×10^{-13}
7000	5.105×10^{-13}	1.171×10^{-12}	1.682×10^{-12}
10000	3.974×10^{-12}	6.773×10^{-12}	1.075×10^{-11}
12000	8.785×10^{-12}	1.392×10^{-11}	2.271×10^{-11}
15000	2.082×10^{-11}	2.859×10^{-11}	4.942×10^{-11}
17000	3.096×10^{-11}	4.010×10^{-11}	7.105×10^{-11}
20000	4.575×10^{-11}	5.804×10^{-11}	1.038×10^{-10}

TABLE S4. N_2 dissociation rates for the $O(^3P) + N_2(X^1\Sigma)$ collisions for 7000 to 20000 K calculated using QCT simulations on the $^3A'$ and $^3A''$ PESs. Units are in $cm^3s^{-1}molecule^{-1}$

T (K)	$k_1^d(^3A') + k_1^d(^3A'')$
7000	0.000
10000	1.061×10^{-13}
12000	5.848×10^{-13}
15000	3.915×10^{-12}
17000	6.888×10^{-12}
20000	1.720×10^{-11}

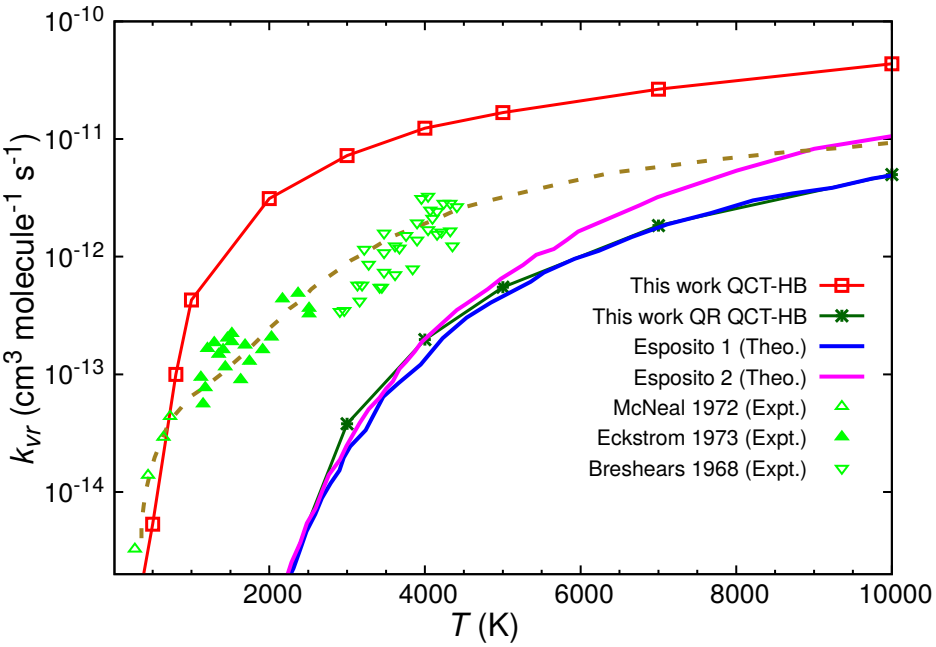

FIG. S2. Vibrational relaxation rates for O + $N_2(\nu = 1) \rightarrow$ O + $N_2(\nu' = 0)$. QR QCT-HB rates calculated from the quasi-reactive (QR) trajectories (see text). The fit to the experimental results is shown as dashed olive line.

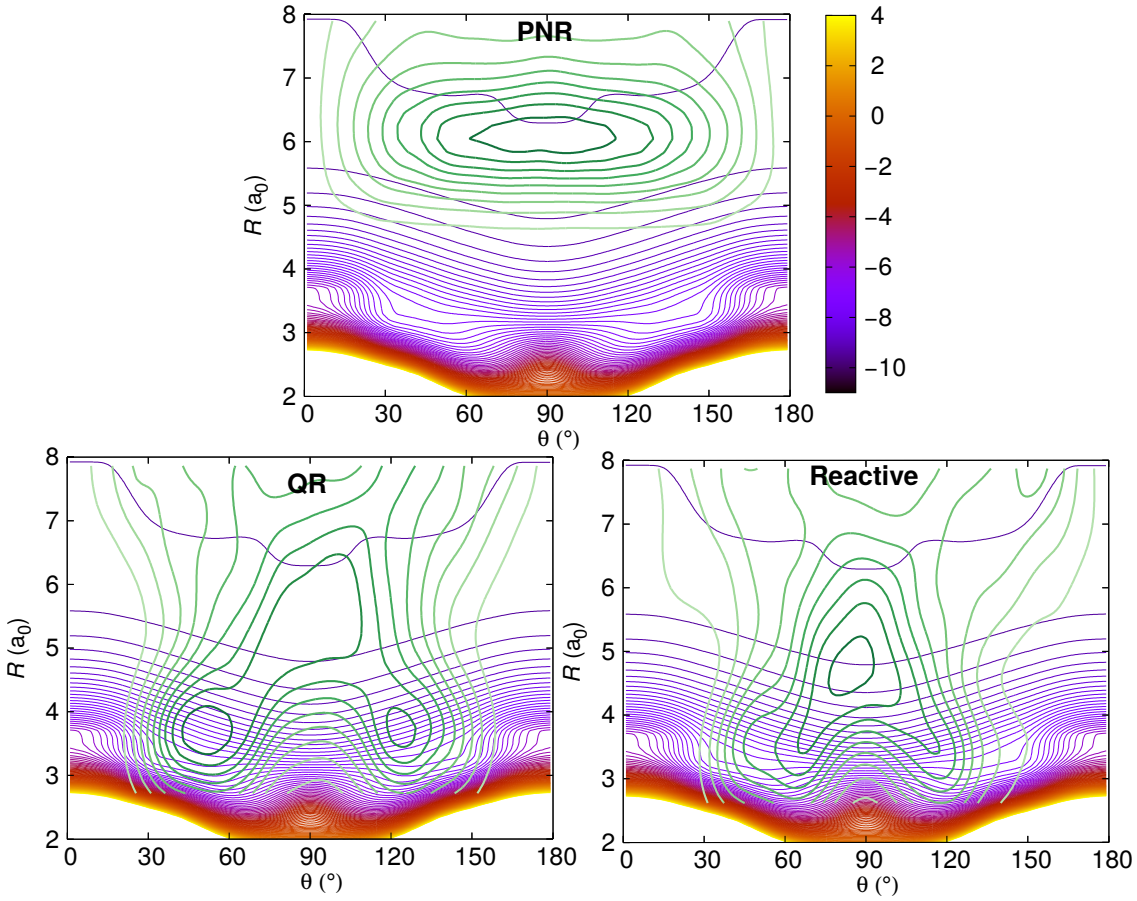

FIG. S3. Conformational sampling (green isocontour lines) for the three different types of trajectories projected onto the relaxed ($0.9 \leq r \leq 1.3$ a_0) O+N_2 PES. 4×10^5 trajectories were run at 4000 K on the $^3A''$ PES, out of which 664, 204 and 60 trajectories were found to be PNR, QR, and reactive trajectories, respectively. The PNR trajectories sample the long range part of the PES (the maximum at $R \approx 6$ a_0) and never enter the strongly interacting region ($R < 4$ a_0) whereas the QR and reactive trajectories heavily sample the strongly interacting region. The distributions have been smoothed by using kernel density estimation (KDE)[1] as implemented in the 'R-studio' package[2]. The contour lines represent 10 % to 90% of the maximum intensity for each case, and dark contours correspond to increased population. It is noted that all distributions are close to converged as they display near-C_{2v} symmetry as required by the underlying PES.

REFERENCES

[1]W. N. Venables and B. D. Ripley, in *Modern Applied Statistics with S* (Springer New York, 2002) pp. 271–300.

[2]R Core Team, *R: A Language and Environment for Statistical Computing*, R Foundation for Statistical Computing, Vienna, Austria (2017).